Int. J. Electrochem. Sci., 3 **(2008)** 416 - 426

International Journal of ELECTROCHEMICAL SCIENCE
www.electrochemsci.org

Electrocatalytic Activities of Pd-Ni Nanoparticles Obtained on Multiwalled Carbon Nanotubes towards Oxygen Evolution in 1M KOH

J. P. Singh[1], *X. G. Zhang*[1], *Hu -lin Li*[1,*], *A. Singh*[2] *and R.N. Singh*[2,**]

[1] College of Material Science and Technology, Nanjing University of Aeronautics and Astronautics, Nanjing – 210016, China
[2] Department of Chemistry, Faculty of Science, Banaras Hindu University, Varanasi – 221005, India
[*]E-mail: lhl_msc@nuaa.edu.cn
[**]E-mail: rnsbhu@rediffmail.com

Received: 9 December 2007 / *Accepted:* 18 January 2008 / *Online published:* 20 February 2008

Pd and Pd-Ni nanoparticles were synthesized on the surface of a new catalytic support, modified multiwalled carbon nanotubes (MWCNTs), by chemical precipitation method at 90^0C and their physicochemical and electrocatalytic properties towards oxygen evolution reaction (OER) in 1M KOH have been investigated using transmission electron microscopy, X-ray diffraction, cyclic and steady state voltammetries. It is observed that introduction of Ni from 0.6 to 1.7 wt% increases the electrocatalytic activity for the OER of the base metal (Pd) attached to the surface of MWCNTs (C) showing the greatest activity with 1.1 wt% Ni (i.e., $PdNi_{0.5}$/C). At E = 0.55 V vs. SCE in 1M KOH at 25^0C, the apparent electrocatalytic activity of the $PdNi_{0.5}$/C (1.1 wt%) electrode(~ 45 $mAcm^{-2}$) was more than 90 times higher than that of the base Pd/C electrode (~ 0.4 $mAcm^{-2}$).

Keywords: Carbon composites, Electrocatalysis, Oxygen evolution reaction, Multiwalled carbon nanotubes

1. INTRODUCTION

The increased applications of single-walled carbon nanotubes (SWCNTs)/ multiwalled carbon nanotubes (MWCNTs) have been found as effective catalyst supports in the field of electrocatalysis and synthesis during recent years [1-3]. It is because of the fact that SWCNTs/MWCNTs have large surface areas and unique structural, electrical, mechanical, electromechanical and physical properties [4-7]. In order to improve the catalytic efficiency to a reasonably high extent, these new catalyst supports were recently produced by different methods [8-14].Carbon nanotubes (CNTs) have been

proposed as an advanced and an ideal material for supporting nanosized metallic particles in the electrodes for electrocatalysis as well as low temperature fuel cells. Attaching transition metal nanoparticles to nanotubes and nanotube sidewalls is of interest to obtain nanotube/nanoparticle hybrid materials with useful properties [15].

A survey of literature reveals that though a large number of pure metals and their alloys and pure as well as mixed oxides have been investigated as electrocatalysts for oxygen evolution reaction (OER) and comprehensively reviewed in books [16-19] and journals [20-33], similar studies appear to have not been made with metals/alloys loaded on MWCNTs. We have obtained coatings of pure Pd and Pd-Ni binary alloys/composites on the surface of MWCNTs by a chemical precipitation method and investigated their physicochemical and electrocatalytic properties in relation to oxygen evolution (OE) in 1M KOH; details of results of the investigation are described in this paper.

2. EXPERIMENTAL PART

2.1. Pretreatment of MWCNTs

The MWCNTs (10 – 20 nm diameter) were produced via the chemical vapor deposition method [14] using methane as carbon source and iron as catalyst. Oxidative treatment of MWCNTs was carried out by refluxing raw of MWCNTs with 4M nitric acid at ~ 150^0C for 5 h. It was then washed thoroughly with deionized water and suspension was separated by centrifugal method and dried under vacuum at 90^0C for 4 h.

2.2 Deposition of metals on MWCNTs

Transitions metals were deposited on MWCNTs by a chemical precipitation method recently reported by Li et al. [34]. For the purpose, MWCNTs were vigorously mixed with appropriate volumes of 20 mM $PdCl_2$ and 20 mM $Ni(NO_3)_2$ solutions in isopropyl alcohol-water (1:3 v/v) solvent mixture at 50^0C for 6 h. The suspension was then heated up to 80^0C and pH was adjusted 8.5 using 0.5M Na_2CO_3 solution. Subsequently, the reducing agent, sodium borohydride ($NaBH_4$) was added in excess to carry out the chemical reduction for 2 h. Pd and Ni get attached to the MWCNTs [6, 7, 14] through the following reactions:

$$PdCl_2 + 2NaBH_4 \longrightarrow Pd + H_2 + 2BH_3 + 2NaCl \text{ ----------[1]}$$

$$Ni(NO_3)_2 + 2NaBH_4 \longrightarrow Ni + H_2 + 2BH_3 + 2NaNO_3 \text{ ---------[2]}$$

The resultant suspension was filtered, washed and vacuum-dried at 90^0C for 4 h to obtain Pd and Ni attached to the MWCNTs.

Following the above method, the composite/alloy of Pd and Ni with five different compositions, as shown in Table1, were attached to the MWCNTs surface. The composition of the composite was varied by changing the ratio of volumes of the two solutions, $PdCl_2$ and Ni $(NO_3)_2$.

Table 1. Pd-Ni alloys description.

Description	Ni : Pd (atomic ratio)	Abbreviation
5 wt% Pd	0	Pd/C
4.4 wt% Pd + 0.6 wt% Ni	0.3	$PdNi_{0.3}$/C
4.2 wt% Pd + 0.8 wt% Ni	0.4	$PdNi_{0.4}$/C
3.9 wt% Pd + 1.1 wt% Ni	0.5	$PdNi_{0.5}$/C
3.3 wt% Pd + 1.7 wt% Ni	1	PdNi/C

All the chemicals were of analytical grade and procured from Beijing Chemical Plant and used without further purification.

2.3. XRD / TEM Analysis

The structural morphology of synthesized nano-composites has been studied by a FEI-Tecnai G2 20 S-TWIN transmission electron microscopy (TEM). Before taking the transmission electron micrographs, the Pd-Ni-MWCNTs composite was first dispersed in the ethanol solution ultrasonically up to 20 minutes, and then the resulting suspension was dropped onto the Cu-grid and observed at 100 KV.

The powder X-ray diffraction (XRD) patterns were recorded on an X-ray diffractometer (Bruker D8 advance-X) in the angle (2θ) range, 20 – 90^0 using Cu-Kα as the radiation source (λ = 0.154056 nm), the scan rate being 4^0 min^{-1} (step: 0.02^0; step time: 0.3 s).

2.4. Preparation of MWCNTs / Pd-Ni composite/alloy electrodes

16 mg of loaded Pd-Ni alloy on MWCNTs was ultrasonically mixed with 0.4 ml of 1wt% Nafion solution (Aldrich, 5 wt% solutions), 0.8 ml deionized water and 1.6 ml ethanol for 20 min. One drop of the resulting suspension (ink) was pipetted onto the Au disk (2mm diameter) substrate. After drying one drop of ink was again pipetted onto the Au substrate and dried overnight. Nafion has a sufficient strength to attach the MWCNTs with particles permanently to the Au electrode [35].

2.5. Electrochemical studies

Electrochemical studies, cyclic and steady state voltammetries (CV), were carried out in a conventional three electrode single compartment glass cell using CHI 660B electrochemical work station (Covarda). The working electrode was Au/MWCNTs/Pd-Ni electrode. The reference and auxiliary electrodes were SCE and pure Pt foil (~ 2 cm^2), respectively. To minimize the IR drop, the tip of reference electrode was set at a distance of about 2 mm from the surface of the working

electrode. All the potentials measured in the study are reported with respect to SCE only. All experiments were performed at 25^0C.

3. RESULTS AND DISCUSSION

3.1. Physicochemical characterization

3.1.1. Transmission electron micrographs analysis

The transmission electron micrographs (TEM) of the two electrodes, namely Pd/C and $PdNi_{0.4}$/C, were recorded and are reproduced in Fig. 1a and Fig. 1b, respectively. It can be seen that the deposits are well dispersed on the MWCNTs support. Further, these deposits look to be preferentially attached to the ends, links and connecting regions of the MWCNTs. Thus, TEM images reveal that the composite of Pd and Ni are in intimate contact with the MWCNTs surface, positioned at the side and top of the tubes. In addition, the density of the deposit was found to be greater on the thicker bundles of MWCNTs than that on the thinner or individual tubes. This may be ascribed to the presence of greater number of carboxylic acid groups on the thick bundles [36].

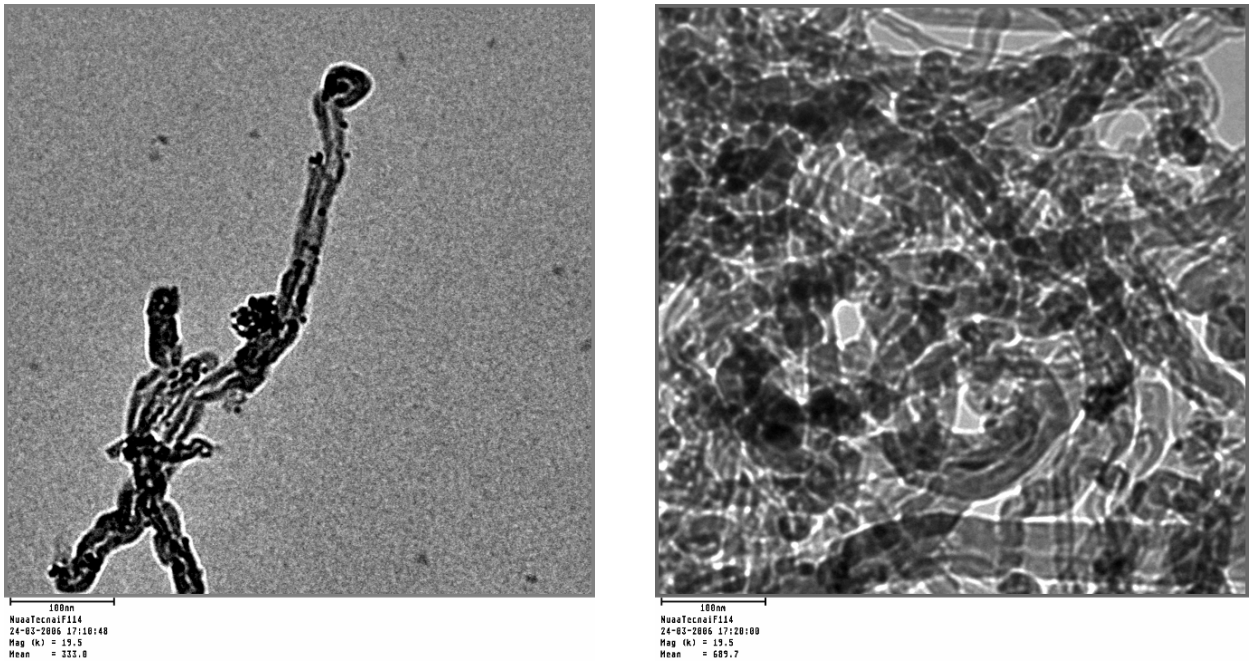

(a) (b)

Figure 1. Transmission electron micrographs (TEM) of (a) Pd loaded on MWCNTs and (b) $PdNi_{0.4}$ alloy loaded on MWCNTs

3.1.2. X-ray diffraction analysis

The X-ray diffraction (XRD) patterns of Pd-Ni-MWCNTs composites are shown in Fig. 2. The five major diffraction peaks have been observed at $2\theta \approx 26.6$, 40, 44.5, 46.7 and 51.8^0. The intense

(002) diffraction peak corresponds to graphite phase (JCPDS file: 25-0284). The diffraction peaks (111) and (200) corresponding to $2\theta = 40$ and 46.7^0, respectively indicate the presence of Pd in the Pd-Ni-MWCNTs composites (JCPDS file: 05-0681) while the peaks corresponding to $2\theta = 44.5$ and 51.85 have the signature of (111) and (200) planes of Ni in the composites of MWCNTs. The standard XRD peaks of Pd and Ni (JCPDS file No. 05-0681 and JCPDS file No. 04-0850) of higher angles were closed to each other and their intensities were also very low. Results of the XRD analyses clearly reveal that the introduction of Pd-Ni layers onto the surfaces of MWCNTs are accomplished by the deposition process, and the phase structure of the deposited Pd-Ni layers is an amorphous state. Further, the prepared nano-composites produced the segregated states of Pd and Ni on MWCNTs and not in the form of Ni-Pd alloy.

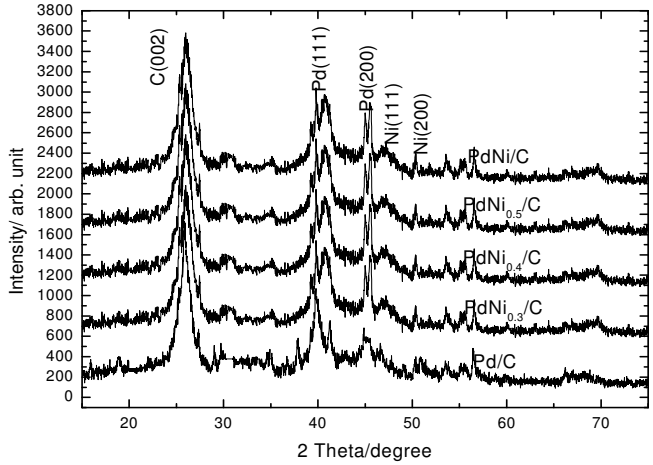

Figure 2. XRD powder patterns of Pd-Ni alloys loaded on MWCNTs at 90^0C.

3.2. Electrochemical properties

3.2.1. Cyclic Voltammetry

Cyclic voltammetry (CV) of each prepared Pd-Ni alloys loaded on MWCNTs including bare Au electrode were recorded at the scan rate of 20 mV s^{-1} in the potential region 0.0 – 0.6 V in 1M KOH at 25^0C. To avoid complexities/overlapping in presentation, CV curves are shown in two Figs. 3 and 4.The nature of these cyclic voltammograms were almost similar; only in the case of bare Au and Pd/C, CV curves appeared different than the rest, because they did not show any surface oxidation-reduction peaks.

Each voltammograms excepting for Pd/C catalytic film shown in Fig. 3 and 4 exhibited a pair of redox peaks (an anodic and a corresponding cathodic peak) prior to the onset of the oxygen evolution reaction (OER). Voltammograms for Pd/C catalytic film did not show any redox peaks. Values of the anodic (E_{pa}) and cathodic (E_{pc}) peak potentials, the peak separation potential ($\Delta E_p = E_{pa}$ -

E_{pc}), the formal redox potential ($E^0 = (E_{pa} + E_{pc})/2$) and the anodic peak current (I_p) were estimated and are listed in Table 2.

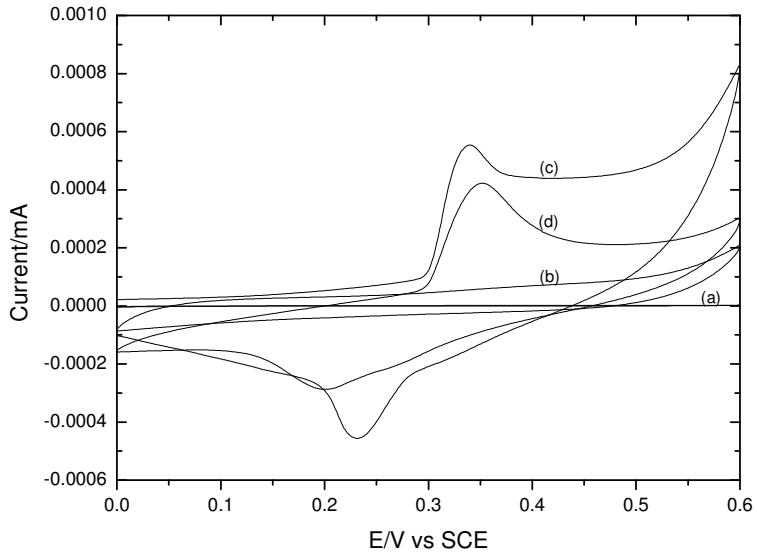

Figure 3. Cyclic Voltammograms of electrodes at 20 mVs^{-1} in 1M KOH at 25^0C; (a): bare Au, (b): Pd/C, (c): $PdNi_{0.3}$/C and (d): PdNi/C alloy.

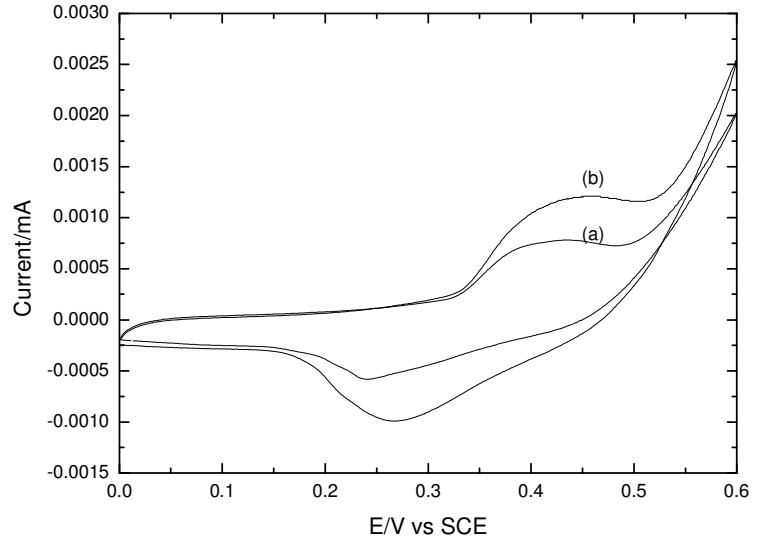

Figure 4. Cyclic Voltammograms of PdNi alloy electrodes at 20 mVs^{-1} in 1M KOH at 25^0C; (a) $PdNi_{0.4}$/C and (b) $PdNi_{0.5}$/C loaded on MWCNTs.

This Table 2 shows that an increase in the Ni concentration from 0.3 to 0.5 mol shifts the E^0 value towards the potential for the commencement of the oxygen evolution (OE). However, the higher

concentration of Ni (i.e. 1.0 mol) appeared to reduce the E^0 value. The similar redox peaks have also been observed in the cyclic voltammetry for Ni in alkaline solution [24, 25]. Thus, the observed redox peaks on the Pd-Ni composite electrodes are mainly due to the formation of the Ni^{2+} / Ni^{3+} redox couple. The effect of the scan rate on the redox peaks has also been studied. In case of each composite electrode, the plot, i_p vs (scan rate)$^{1/2}$, was found to be linear. A set of six voltammograms determined at varying scan rates vis-a-vis 'i_p vs (scan rate)$^{1/2}$' plot in case one composite electrode, PdNi/C, are given in Figs. 5 and 6, respectively. The results show that the redox surface process concerning the formation of Ni^{2+}/ Ni^{3+} is diffusion controlled [14].

Table 2. Results of the cyclic voltammetry of Pd-Ni alloy loaded on MWCNTs in 1M KOH at 20 mV s^{-1} and 25 ^{0}C.

Electrode	E_{Pa} (mV)	E_{Pc} (mV)	$\Delta Ep=E_{Pa}-E_{Pc}$ (mV)	$E^0=(E_{Pa}+E_{Pc})/2$ (mV)	Anodic peak current density (mA cm^{-2})
Au	-----	-----	-----	-----	-----
Pd/C	-----	-----	-----	-----	-----
$PdNi_{0.3}$/C	341	231	110	286	17.57
$PdNi_{0.4}$/C	437	240	197	339	24.90
$PdNi_{0.5}$/C	457	271	186	364	38.66
PdNi/C	353	200	153	277	13.44

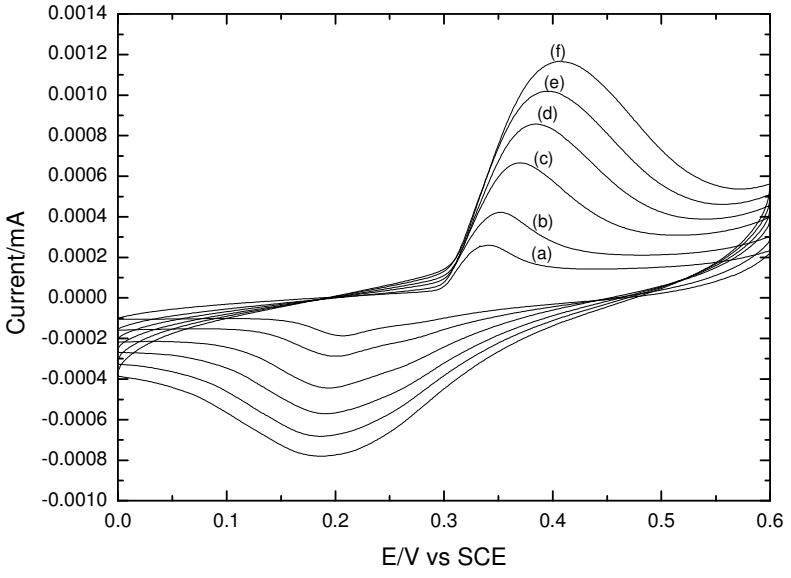

Figure 5. Cyclic Voltammograms of the PdNi alloy electrode at different scan rates in 1M KOH at 25^0 C: (a): 10 mV s^{-1}, (b): 20 mV s^{-1}, (c): 40 mV s^{-1}, (d): 60 mV s^{-1}, (e): 80 mV s^{-1} and (f): 100 mV s^{-1}

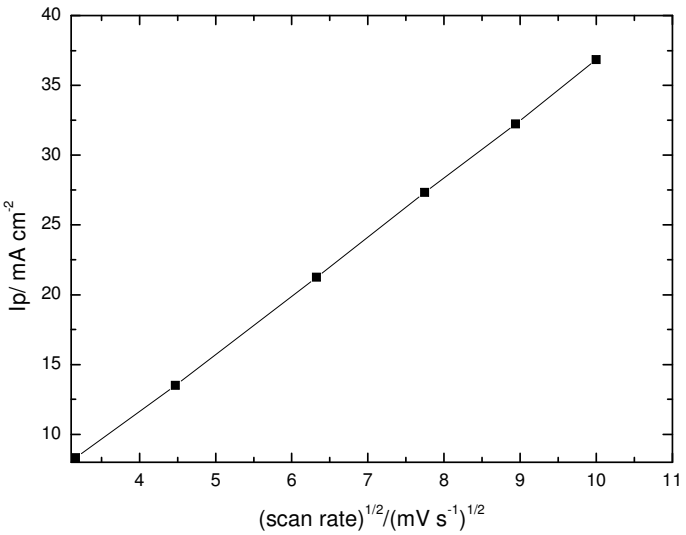

Figure 6. Ip vs (scan rate)1/2 plot for the PdNi/C electrode.

3.2.2. Electrocatalytic Activity

To determine the electrocatalytic activity for the OER, the potentiostatic polarization curves (E vs. log i) have been recorded for each electrocatalyst at a slow scan rate (0.2 mV s^{-1}) in the potential region 0.40- 0.8 V in 1M KOH at 25^0C and curves, so obtained, are reproduced in Fig. 7. Features of E vs. log i curves for Pd-Ni composites were almost similar. The Tafel slopes at low potentials ranged between ~ 60 and ~150 mVdecade^{-1}At the higher potentials (> 0.65V), each E vs. log i curve gets polarized, this is possibly due to the sticking of O_2 -gas bubbles at the surface of the electrode.

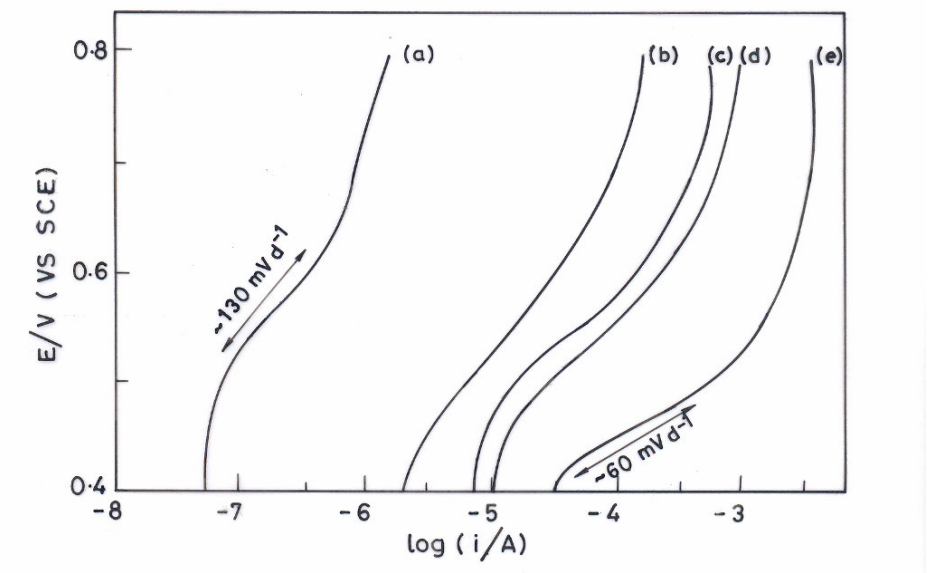

Figure 7. Tafel plots for Pd-Ni alloys loaded on MWCNTs at a scan rate of 0.2 mV s^{-1} in 1M KOH at 25^0 C: (a): bare Au, (b): Pd, (c): $PdNi_{0.3}$, (d): $PdNi_{0.4}$ & (e): $PdNi_{0.5}$

To compare the electrocatalytic activity, i value at a constant potential, E = 0.55 V vs. SCE for each electrocatalyst was noted from Fig.7 and the same has been displayed in Table 3. This Table shows that with the increase in the Ni content in the composite loaded on MWCNTs the apparent current density (i_a) increases, reaches maximum at 0.5 mol Ni (i_a ~ 45 mA cm^{-2}) and decreases thereafter, i.e. at 1.0 mol Ni (i_a ~ 1.5 mA cm^{-2}).

Table 3. Electrode Kinetic Parameters for Oxygen Evolution Reaction on Pd-Ni alloys loaded on MWCNTs in 1M KOH at 25^0C.

Electrode	Tafel slope $mVdecade^{-1}$	Apparent current density (i_a) (mA cm^{-2}) at E = 0.55V	Specific activity (SA) (mA mC^{-1})
Au	~140	0.003	-----
Pd/C	~150	0.49	-----
$PdNi_{0.3}$/C	~120	1.55	5.02
$PdNi_{0.4}$/C	~60	3.18	5.64
$PdNi_{0.5}$/C	~77	45.54	5.83
PdNi/C	~120	1.55	1.35

The specific activity (SA) of the Pd-Ni alloy loaded on MWCNTs for OER (Table 3) was also calculated using the relation [37],

$$SA = i/Q \text{ ---------- [3]},$$

where i, is the peak current density obtained from forward CV scan shown in Figs. 3 and 4, and Q is the corresponding charge. A similar effect of the variation of Ni content in the Pd-Ni alloy on the specific activity was also observed as was already found on the apparent current density. However, the effect of Ni content on the specific activity is not very significant, which demonstrates that Ni introduction does not significantly improve the electronic properties of the composite. So, the change in the apparent electrocatalytic activity of the composite electrode with Ni introduction is mainly due to modification in the geometrical properties (surface area) of the material. Based on values of 'i_a' at E = 550 mV in 1M KOH at 25^0C, the different electrocatalysts can be placed in the following catalytic order:

$$PdNi_{0.5}/C > PdNi_{0.4}/C > PdNi_{0.3}/C > PdNi/C > Pd/C > Au$$

The similar order for the peak current densities (Table2) was also found. Values of the peak current density were the greatest with the $PdNi_{0.5}$/C electrode while it was the lowest with the PdNi/C electrode. The small variation in the peak potentials and shapes of the redox peaks may be ascribed to compositional/structural changes in electrochemically active materials [38].

4. CONCLUSIONS

The study presents a novel method for preparing highly dispersed Pd and Ni particles on MWCNTs surfaces for the OER. Result show that small addition of Ni greatly enhances the electrocatalytic activity of the composite; the observed j_a value being ~ 90 times higher for the $PdNi_{0.5}$ composite at E = 0.55V in 1M KOH than that of the base Pd/C electrode. Efforts are continued to enhance the activity of the composite further by introducing Fe and /or Co in the composite.

ACKNOWLEDGEMENTS
One of the authors (J P S) is thankful to the administration of Nanjing University of Aeronautics and Astronautics, Nanjing for providing financial support as postdoctoral fellow to carry out the investigation.

References

1. J. Prabhuram, T.S. Zhao, Z.X. Liane, R. Chen, *Electrochim, Acta* 52 (2007 2649.
2. J.S. Ye, H.F. Cui, Y. Wen, W.D. Zhang, G.Q. Xu, F.S. Sheu, *Microchimica Acta* 152 (2006) 267.
3. G.P. Jin, Y.F. Ding, P.P. Zheng*, J. Power Sources* 166 (2007) 80.
4. M.A. Hayat, In: 'Colloidal Gold: Principles, Methods and Applications', vols. 1 and 2, Academic Press, San Diego, 1989.
5. D.L. Feldheim, C.A. Foss, In: 'Metal nanoparticles: synthesis, characterization and applications', Marcel Dekker, New York, 2002.
6. S. Iijima, *Nature* 354 (1991) 56.
7. Z. Liu, X. Lin, J.Y. Lee, W. Zhang, M. Han, L.M. Gan, *Langmuir* 18 (2002) 4054.
8. A. Sartre, M. Phaner, L. Porte, G..N. Sauvion, *Appl. Surf. Sci*. 70 (1993) 402.
9. X.Q. Tong, M. Aindow, J.P.G. Tarr, *J. Electroanal. Chem*. 395 (1995) 117.
10. A.M. Polcaro, S. Palmas, *Electrochim. Acta* 36 (1991) 921.
11. C.K. Lai, Y.Y. Wang, C.C. Wan, *J. Electroanal. Chem* 322 (1992) 267.
12. L.R. Radovic, F. Rodriguez-Reinoso, Carbon materials in catalysis, Thrower P A. Editor, In 'Chemistry and physics of carbon', vol 25, N Y; Dekker: p. 243.
13. D.J. Guo, H.L. Li, *J. Electroanal. Chem*. 573 (2004) 197.
14. D.J. Guo, H.L. Li, *J. Colloid Interface Sci*. 286 (2005) 274.
15. J. Kong, M. Chapline, H. Dai, *Adv. Mater*. 13 (2001) 1384.
16. S. Trasatti, In 'The Electrochemistry of Novel Materials', Eds. J. Lipkowsky and N. Philip Ross, editor, VCH Publishers Inc., New York, 1994, p. 207.
17. E.J.M.O' Sullivan, E.J. Calvo, in 'Comprehensive Chemical kinetics', vol. 27, Eds., R.G. Compton. Elsevier, Amsterdam, 1987; p. 274.
18. L.D. Burke, in S. Trasatti (Ed.) Electrodes of Conductive metallic oxides Part A, Elsevier, Amsterdam, 1980; p. 141.

19. L.G. Tejuca, J.L.G. Fierro, J.M. Tascon, In 'Advances in Catalysis', vol. 36. (edited by D.D. Eley, H. Pines, P.B. Wiesz), Academic Press, N. Y., 1989; p.237.
20. R.N. Singh, J.P. Singh, B. Lal, M.J.K. Thomas, S. Bera, *Electrochim. Acta* 51 (2006) 5515.
21. M. Hamdani, M.I.S. Pereira, J. Douch, A. Ajit Addi, Y. Berghoute, M.H. Mendonca, *Electrochim. Acta* 49 (2004) 1555.
22. B. Marsan, N. Fradette, G. Beaudoin, *J. Electrochem. Soc*. 137 (1992) 1889.
23. M. De Koninck, S.-C. Poirier, B. Marsan, *J. Electrochem. Soc*. 153 (2006) A2103.
24. F. Svegl, B. Orel, I. Grabec-Svegl, V. Kaucie, *Electrochim. Acta* 45 (2000) 4359.
25. X. Wang, H. Luo, H. Yang, P.J. Sebastian, S.A.Gamboa, *Int. J. Hydrogen Energy* 29 (2004) 967.
26. G. Spinolo, S. Ardizzone, S. Trasatti, *J. Electroanal. Chem*. 423 (1997) 497.
27. R.N. Singh, N.K. Singh, J.P. Singh, *Electrochim. Acta* 47 (2002) 3873.
28. A.N. Jain, S.K. Tiwari, P. Chartier, R.N. Singh, *J. Chem. Faraday Trans*. 91 (1995)1871.
29. G. Wu, N. Li, De-R. Zhou, K. Mitsuo, Bo-Q. Xu, *J. Solid State Chem*. 177 (2004) 3682.
30. Bo. Chi, J. Li, X. Yang, H. Lin, N. Wang, *Electrochim. Acta* 50 (2005) 2059.
31. J.O'M. Bockris, T. Otagawa, *J. Phy. Chem*. 87 (1983) 2960.
32. P. Nkeng, G. Poillerat, J.F. Koeing, P. Chartier, B. Lefez, J. Lopitaux, M. Lenglet, *J. Electrochem. Soc.* 142(6) (1995) 1777.
33. A.C. Tavares, M.A.M. Cartaxo, M.I.Da Silva Pereira, F.M. Costa, *J. Electroanal. Chem*. 464 (1999) 187.
34. X. Li, I.M. Hsing, *Electrochim. Acta* 51 (2006) 5250.
35. A. Pozio, M.D. Francesco, A. Cemmi, F. Cardellini, L. Giorgi, *J. Power Sources* 105 (2002) 13.
36. Z.F. Liu, Z.Y. Shen, T. Zhu, S.F. Hou, L.Z. Ying, Z.J. Shi, Z.N.Gu, *Langmuir* 16 (2000) 3569.
37. D. Pan, J. Chen, W. Tao, L. Nie, S. Yao, *Langmuir* 22 (2006) 5872.
38. S. Trasatti, *Electrochim. Acta* 36 (1991) 225.